Macromolecules
ARTICLE

Macromolecules **2010**, *43*, 2759–2771
DOI: 10.1021/ma902110v

Synthesis and Characterization of New Self-Assembled Metallo-Polymers Containing Electron-Withdrawing and Electron-Donating Bis(terpyridine) Zinc(II) Moieties

Florian Schlütter,[†] Andreas Wild,[†,‡] Andreas Winter,[‡,§] Martin D. Hager,[†,‡] Anja Baumgaertel,[†,‡] Christian Friebe,[†,‡] and Ulrich S. Schubert*[,†,‡,§]

[†]*Laboratory of Organic and Macromolecular Chemistry, Friedrich-Schiller-University Jena, Humboldtstr. 10, 07743 Jena, Germany,* [‡]*Dutch Polymer Institute (DPI), P.O. Box 902, 5600 AX Eindhoven, The Netherlands, and* [§]*Laboratory of Macromolecular Chemistry and Nanoscience, Eindhoven University of Technology, P.O. Box 513, 5600 MB Eindhoven, The Netherlands*

Received September 26, 2009; Revised Manuscript Received January 17, 2010

ABSTRACT: A series of rigid π-conjugated bis(terpyridines) (**M1−M7**) bearing electron-acceptor spacer units in 4′-position was synthesized in moderate to high yields by Pd^0-catalyzed Sonogashira cross-coupling reactions. The compounds were fully characterized by NMR spectroscopy, MALDI−TOF mass spectrometry, elemental analysis and their photophysical properties were discussed in detail. These new bis(terpyridines) were applied for the self-assembly reaction with Zn^{II} ions to form metallo-homo polymers (**P1−P7**). Broadened NMR signals and UV−vis titration experiments confirmed the successful polymerization. The electro-optical properties of the materials were investigated in detail. Band gaps up to 2.08 eV and bright blue to orange photoluminescence with quantum yields of 18 to 66% were observed strongly depending on the nature of the π-conjugated bis(terpyridine) system. In combination with electron-donor ditopic terpyridine ligands (**MD1** and **MD2**), two Zn^{II} random copolymers (**R1** and **R2**) were synthesized. These materials were investigated by UV−vis absorption and photoluminescence experiments in dilute solution and in the solid state, prepared by spin-coating from DMF solutions. Thereby, random copolymer **R2** featured an energy transfer from the donor to the acceptor part in dilute solution.

Introduction

In the extensive search for new materials for optoelectronic applications, metal−ligand coordination has gained much interest in the last decades.[1−3] By varying the metal−ligand combination, the properties of such supramolecular assemblies can be tuned, not only with respect to their binding strength, reversibility and solubility, but also with respect to their optoelectronic properties.[4−10]

Therefore, several *N*-heterocyclic ligands, e.g., 2,2′-bipyridine, 1,10-phenanthroline, and, in particular, [2,2′:6′,2″]-terpyridine, attracted much interest as supramolecular templates due to their high binding affinity towards many transition metal ions in low oxidation states, through dπ−pπ* bonding and the prevention of Δ/Λ-chirality compared to 2,2′-bipyridine metal complexes.[11,12] This work focuses on [2,2′:6′,2″]-terpyridines bearing π-conjugated substituents in 4′-position,[8,12−15] which are showing interesting photophysical as well as electrochemical properties. Furthermore, bis(terpyridines) allow the electronic communication between the metal-complexed terpyridine units pointing out their potential in the design of functional materials.[9,10,16−19] In combination with transition metal ions [2,2′:6′,2″]-terpyridines form distorted octahedral complexes showing different stabilities from kinetically inert (e.g., Ru^{II} and Ni^{II}) to labile (e.g., Zn^{II}).[10,20] With respect to this, the availability and the low costs of zinc(II) ions show a considerable advantage compared with the other potential metals.

Such metal complexes have found numerous applications as luminescent sensors in molecular biology and medical diagnostics, as photocatalysts, effective materials in self-assembled molecular devices as well as molecular wires.[21,22] The combination of the properties of $[M(tpy)_2]^{2+}$ complexes (i.e., optical, electrochemical, magnetic properties) with the versatile properties of organic polymers (i.e., mechanical properties, solubility, processability) leads to fascinating possibilities.[2,23−25] The group of Constable and Thompson developed an approach for the utilization of ditopic [2,2′:6′,2″]-terpyridines as building blocks for the self-assembly with transition metal ions to metallo-polymers and -oligomers.[26] Beside highly stable Ru^{II} metallo-polymers, Zn^{II} terpyridine metallo-polymers gained recently interest due to their well-defined structures and enhanced photo- and electroluminescent properties at room temperature.[23,27,28] Therefore, Zn^{II} containing metallo-polymers are promising materials for potential applications, e.g., in organic light-emitting diodes (OLED). Such systems provide large equilibrium constants, which are essential for the thermodynamic driven polymer formation.[9,10,29] In previous work in this field, the group of Würthner showed the metal-directed self-assembly of highly fluorescent [2,2′:6′,2″]-terpyridine bearing perylene bisimdide in 4′-position to photoactive metallo-polymers and presented their spectroscopic and structural properties.[9,19] Lin et al. applied fluorene substituted ditopic [2,2′:6′,2″]-terpyridines for the synthesis of Zn^{II} containing metallo-homopolymers and metallo-*alt*-copolymers.[23,28] According to Che and Cao, the incorporation of [2,2′:6′,2″]-terpyridine Zn^{II} moieties into different main-chain structures leads to a variety from violet to yellow colors with high PL quantum yields.[30,31] Furthermore, we

---

*Author for correspondence. Telephone: +49(0) 3641 948200. Fax: +49(0) 3641 948202. E-mail: ulrich.schubert@uni-jena.de.

showed several types of bis(terpyridines) bearing electron-donating π-conjugated spacer units with remarkable photophysical properties and used them as building blocks for the construction of Zn^{II} containing metallo-polymers.[24,32,33] We could improve the film-forming ability of such systems by incorporating polymer side-chains to π-conjugated bis(terpyridines).[16]

In continuation of this work, we focused on the synthesis of bis(terpyridine) building blocks with electron-accepting π-conjugated spacer units, which should significantly influence the optical properties and, lead in combination with the established electron-donor units, towards supramolecular low band gap materials.[34] Potential photovoltaic materials, e.g., π-conjugated systems, have to cover the red and near-infrared ranges of the terrestrial solar spectrum, based on the maximum photon flux density of the sunlight, located at approximately 700 nm (bandgap, $E_g \approx 1.77$ eV). Hence, it is desirable to develop π-conjugated systems with broader absorptions by reducing their E_g values.[35] The combination of electron-acceptors with electron-donors leads to a significant decrease of the distance (bandgap, E_g) between the highest occupied molecular orbital (HOMO) of the donor and the lowest unoccupied molecular orbital (LUMO) of the acceptor, which results in a bathochromic shift of the absorption.[34,35] Therefore, we attached well-known strong electron-acceptors, e.g., [2,1,3]benzothiadiazole, terephthalates, thieno[3,4-*b*]pyrazine, quinoxaline as well as a nitrile-groups containing system to the [2,2′:6′,2″]-terpyridine in 4′-position using the Pd^0-catalyzed *Sonogashira* cross-coupling reaction.

These ditopic ligands were polymerized via the coordination of Zn^{II} ions into the corresponding metallo-homo polymers. Furthermore, two statistical metallo-random polymers were synthesized in combination with ditopic terpyridine ligands containing π-conjugated electron-donating spacers. This combination should lead to a transfer of energy from the excited donor part to the acceptor moiety, which can consequently relax under emission. The investigation of energy as well as electron transfer processes is crucial for the understanding of the photosynthetic processes and the design of artificial light-to-energy conversion systems.[36,37] Besides that, an efficient energy transfer process allows long-range information transmission, which could be applied in the development of molecular devices and machines for information technology.[38]

The photophysical and electrochemical properties of the new type of bis(terpyridines) and their corresponding metallo-polymeric materials are discussed in detail.

Experimental Section

Materials and General Experimental Details. All chemicals were purchased from Aldrich, Acros Organics and Alfa Aesar and were of reagent grade and used as received, unless otherwise specified. The solvents were purchased from Biosolve, Aldrich and Acros Organics and were dried and distilled according to standard procedures. Chromatographic separation was performed with standardized silica gel 60 (Merck) and aluminum oxide 90 neutral (Molekula). The reaction progress was controlled by thin layer chromatography (TLC) using aluminum sheets precoated with silica gel 60 F_{254} (Merck) and aluminum oxide 60 F_{254} neutral (Macherey-Nagel).

4′-(4-Ethynylphenyl)-[2,2′:6′,2″]terpyridine (**A**),[39−41] 4,7-dibromo-[2,1,3]benzothiadiazole (**1**),[42] dioctyl 2,5-dibromo-terephthalate (**2**),[43] 5,8-dibromo-2,3-bis(2-ethylhexyl)quinoxaline (**3**),[44,45] (2*Z*,2′*Z*)-3,3′-(2,5-dibromo-1,4-phenylene)bis(2-(4-(2-ethylhexyloxy)phenyl)acrylonitrile) (**4**),[46,47] 5,7-dibromo-2,3-bis(4-(octyloxy)phenyl)thieno[3,4-*b*]pyrazine (**5**),[48,49] tetraoctyl 5,5′-([2,1,3]benzothiadiazole-4,7-diylbis(ethyne-2,1-diyl))bis(2-bromoterephthalate) (**6**), and tetraoctyl 5,5′-(2,5-bis(octyloxy)-1,4-phenylene)bis(ethyne-2,1-diyl)bis(2-bromoterephthalate) (**7**) were prepared according to the literature (see the Supporting Information for the detailed synthetic procedures and characterization). The synthesis of 4′-(4-((1*E*,7*E*)-4-(2-(4-(2-(4-((*E*)-4-([2,2′:6′,2″]terpyridine-4′-yl)-styryl)phenyl)ethynyl)-2,5-bis(2-ethylhexyloxy)phenyl)ethynyl)-styryl)-phenyl)-[2,2′:6′,2″]terpyridine (**MD1**) and 2,7-bis((4-([2,2′:6′,2″]terpyridine-4′-yl)phenyl)ethynyl)-9,9-bis(octyloxy)-*9H*-fluorene (**MD2**) as well as their Zn^{II} metallo-homo polymers is reported elsewhere.[50]

Instrumentation. 1D (^{1}H, ^{13}C) and 2D (^{1}H−^{1}H gCOSY, HSQC, HMBC) nuclear magnetic resonance (NMR) spectra were recorded on a Bruker Cryomagnet BZH 400 (400 MHz), Bruker AC 300 (300 MHz) or Bruker AC 250 (250 MHz) instrument at 298 K. Chemical shifts are reported in parts per million (ppm, δ scale) relative to the residual signal of the deuterated solvent. Coupling constants are given in Hz. UV−vis absorption and photoluminescence (PL) emission spectroscopy were performed on an Analytik Jena SPECORD 250 and Jasco FP-6500 spectrometer, respectively, at 298 K. Absolute photoluminescence quantum yields were evaluated at 298 K on a Hamamatsu photonic multi-channel analyzer C 10027. For these techniques $10^{-6}-10^{-5}$ M solutions in chloroform or *N,N*-dimethylformamide (DMF) were used. Matrix-assisted laser desorption/ionization time-of-flight (MALDI−TOF) mass spectra were obtained from an Ultraflex III TOF/TOF mass spectrometer with dithranol as matrix in reflector as well as linear mode. Elemental analyses were carried out on a CHN-932 Automat Leco instrument. Cyclic voltammetry (CV) measurements were performed using a PA4 polarographic analyzer (Laboratory instruments, Prague, Czech Republic) with a three electrode cell. Platinum (Pt) wire electrodes were used as both working and counter electrodes and a nonaqueous Ag/Ag^I electrode (Ag in 0.1 M $AgNO_3$ solution) was used as reference electrode. Thin films coated onto Pt electrodes from acetonitrile solutions containing 0.1 M tetra-*n*-butylammonium hexafluorophosphate ($(TBA)PF_6$) were used for these measurements. All measurements and film preparations were performed under nitrogen atmosphere within a glovebox. Polymer thin films were prepared by spin-coating polymer solutions from DMF (20 mg/mL) using a spin-coating rate of 1000 rpm for 100 s onto silica fused substrates for optical studies. The glass slides were ultrasonicated in 2% Helmanex-solution (Helma) and 2-propanol for 20 min, in between washed 12 times with distilled water, and finally placed into an ethanol solution and dried using nitrogen. UV−vis absorption and PL emission spectra of these thin films were measured with a Hitachi F-4500 fluorescence spectrophotometer. Layer thicknesses were measured outside the glovebox using a KLA-Tencor P-10 profilometer.

General Procedure for the Synthesis of the Bis(terpyridine) Monomers (M1−M7). To an argon-degassed mixture of 4′-(4-ethynylphenyl)-[2,2′:6′,2″]terpyridine (**A**, 0.50 mmol) and an aromatic bromide (**1**−**7**, 0.25 mmol) in dry THF (30 mL) and dry triethylamine or diisopropylamine (10 mL) were added tetrakis(triphenylphospine)palladium(0) (10 mol %) and copper(I) iodide (10 mol %), and the reaction mixture was refluxed until TLC indicated complete conversion (5 to 48 h). After the reaction had cooled to room temperature, the precipitated ammonia salt was filtered off and washed intensively with THF. Subsequently, dichloromethane was added and the solution was washed with saturated aqueous NH_4Cl/EDTA solution and dried over anhydrous $MgSO_4$. After removal of the solvents, the product was precipitated from methanol. Further purification was achieved by column chromatography (aluminum oxide, CH_2Cl_2 as eluent).

4,7-Bis((4-([2,2′:6′,2″]terpyridine-4′-yl)phenyl)ethynyl)[2,1,3]-benzothiadiazole (M1). According to the above-mentioned general procedure, **M1** was obtained after filtration from the reaction mixture, intensive washing with water and repeated recrystallization from large amounts of chloroform as orange solid (169 mg, 85%). ^{1}H and ^{13}C NMR spectra could not be obtained due to the very low solubility of **M1** in organic solvents. MALDI−TOF MS (dithranol): m/z = 799.25 (100%, $[M + H]^+$). Anal. Calcd for $C_{52}H_{30}N_8S$: C, 78.18; H, 3.78; N, 14.03; S, 4.01. Found: C, 77.98; H, 4.02; N, 14.21; S, 3.76.

Dioctyl 2,5-Bis((4-([2,2′:6′,2″]terpyridine-4′-yl)phenyl)ethynyl)terephthalate (M2). According to the above-mentioned general procedure, **M2** was obtained as a yellow solid (184 mg, 70%). ^{1}H NMR (CDCl$_3$, 300 MHz, δ): 0.84 (m, 6H, CH$_3$), 1.19−1.51 (m, 20H, CH$_2$), 1.78−1.88 (m, 4H, OCH$_2$−CH$_2$), 4.44 (m$_c$, 4H, O−CH$_2$), 7.37 (m$_c$, 4H, H$^{5,5''}$), 7.73 (d, ^3J = 7.5 Hz, 4H, H^{a,b}), 7.88 (m$_c$, 8H, H$^{4,4''}$, H^{a,b}), 7.95 (d, ^3J = 7.5 Hz, 4H, H^{a,b}), 8.26 (s, 2H, H^{A}), 8.69 (d, ^3J = 7.8 Hz, 4H, H$^{3,3''}$), 8.75 (d, ^3J = 3.9 Hz, 4H, H$^{6,6''}$), 8.76 (s, 4H, H$^{3',5'}$). ^{13}C NMR (CDCl$_3$, 75 MHz, δ): 14.1 (CH$_3$), 22.6, 26.1, 28.7, 29.2, 29.3, 31.8 (CH$_2$), 66.1 (O−CH$_2$), 89.0 (C≡C), 96.4 (C≡C), 118.7 (≡C−C), 121.4, 122.9, 123.6, 123.9, 127.3, 132.4, 134.5, 136.1, 136.9, 138.8, 149.2, 149.3, 156.1, 156.1 (C^{aryl}), 165.1 (C=O). MALDI−TOF MS (dithranol): m/z = 1053.51 (100%, [M + H]$^+$). Anal. Calcd for $C_{70}H_{64}N_6O_4$: C, 79.82; H, 6.12; N, 7.98. Found: C, 79.45; H, 6.46; N, 7.79.

2,3-Bis(2-ethylhexyl)-5,8-bis((4-([2,2′:6′,2″]terpyridine-4′-yl)phenyl)ethynyl)quinoxaline (M3). According to the above-mentioned general procedure, **M3** was obtained as a yellow-orange solid (164 mg, 65%). ^{1}H NMR (CDCl$_3$, 300 MHz, δ): 0.87 (m$_c$, 6H, CH$_3$), 1.00 (m$_c$, 6H, CH$_3$), 1.23−1.58 (m, 16H, CH$_2$), 2.31 (m$_c$, 2H, ^{t}C−H), 3.05 (d, ^3J = 6.9 Hz, 4H, N=C−CH$_2$), 7.38 (m$_c$, 4H, H$^{5,5''}$), 7.81 (d, ^3J = 8.4 Hz, 4H, H^{a,b}), 7.91 (m$_c$, 10H, H$^{4,4''}$, H^{a,b}, H^{A}), 7.98 (d, ^3J = 8.4 Hz, 4H, H^{a,b}), 8.70 (d, ^3J = 8.1 Hz, 4H, H$^{3,3''}$), 8.76 (d, ^3J = 4.2 Hz, 4H, H$^{6,6''}$), 8.79 (s, 4H, H$^{3',5'}$). ^{13}C NMR (CDCl$_3$, 75 MHz, δ): 11.0, 14.1 (CH$_3$), 23.1, 26.0, 28.9, 32.9 (CH$_2$), 38.1 (^{t}CH), 39.1 (N=C−C), 88.5 (C≡C), 96.7 (C≡C), 118.7 (≡C−C), 121.4, 123.1, 123.9, 124.3, 127.3, 131.8, 132.4, 136.9, 138.4, 140.9, 149.2, 149.4, 156.1, 156.2, 157.4 (C^{aryl}). MALDI−TOF MS (dithranol): m/z = 1017.53 (100%, [M + H]$^+$). Anal. Calcd for $C_{70}H_{64}N_8$: C, 82.64; H, 6.34; N, 11.01. Found: C, 82.85; H, 5.97; N, 11.01.

3-(4-(1-Cyano-2-(4-(2-ethylhexyloxy)phenyl)vinyl)-2,5-bis((4-([2,2′:6′,2″]terpyridine-4′-yl) phenyl)ethynyl)phenyl)-2-(4-(2-ethylhexyloxy)phenyl)acrylonitrile (M4). According to the above-mentioned general procedure, **M4** was obtained as a yellow-orange solid (187 mg, 72%). ^{1}H NMR (CDCl$_3$, 300 MHz, δ): 0.95 (m$_c$, 12H, CH$_3$), 1.22−1.58 (m, 16H, CH$_2$), 1.75 (m$_c$, 2H, ^{t}C−H), 3.94 (m$_c$, 4H, O−CH$_2$, *E*+*Z* isomers), 6.88−7.06 (d, ^3J = 8.4 Hz, 4H, H^{a,b}), 7.37 (m$_c$, 8H, H$^{5,5''}$, H^{a,b}), 7.73 (d, ^3J = 5.7 Hz, 4H, H^{a,b}), 7.90 (m$_c$, 8H, H$^{4,4''}$, H^{a,b}), 8.06 (s, 2H, H^{A}), 8.46−8.54 (s, 2H, C=C−H^{B}, *E*+*Z* isomers), 8.69 (d, ^3J = 8.4 Hz, 4H, H$^{3,3''}$), 8.77 (m$_c$, 8H, H$^{6,6''}$, H$^{3',5'}$). ^{13}C NMR (CDCl$_3$, 75 MHz, δ): 11.1, 14.1 (CH$_3$), 23.0, 23.8, 29.1, 30.5 (CH$_2$), 39.4 (^{t}CH), 70.8 (O−CH$_2$), 88.0 (C≡C), 97.9 (C≡C), 114.2 (≡C−C), 115.1, 115.2, 117.5, 118.7, 118.8, 121.4, 123.1, 123.9, 126.3, 127.5, 127.6, 131.0, 132.1, 132.3, 132.5, 135.7, 136.3, 137.0, 139.0, 149.1, 156.1 (C^{aryl}), 160.9 (O−C=). MALDI−TOF MS (dithranol): m/z = 1251.69 (100%, [M + H]$^+$). Anal. Calcd for $C_{86}H_{74}N_8O_2$: C, 82.53; H, 5.96; N, 8.95. Found: C, 82.18; H, 5.58; N, 8.56.

2,3-Bis(2-ethylhexyl)-5,7-bis((4-([2,2′:6′,2″]terpyridine-4′-yl)phenyl)ethynyl)thieno[3,4-*b*]pyrazine (M5). According to the above-mentioned general procedure, **M5** was obtained as a red solid (225 mg, 75%). ^{1}H NMR (CDCl$_3$, 300 MHz, δ): 0.90 (m$_c$, 6H, CH$_3$), 1.23−1.31 (m, 20H, CH$_2$), 1.78−1.88 (m, 4H, OCH$_2$−CH$_2$), 4.00 (m$_c$, 4H, O−CH$_2$), 6.88 (d, ^3J = 9.0 Hz, 4H, H^{a,b}) 7.40 (m$_c$, 4H, H$^{5,5''}$), 7.56 (d, ^3J = 8.7 Hz, 4H, H^{a,b}), 7.78 (d, ^3J = 8.4 Hz, 4H, H^{a,b}), 7.90 (m$_c$, 4H, H$^{4,4''}$), 7.97 (d, ^3J = 8.4 Hz, 4H, H^{a,b}), 8.70 (d, ^3J = 7.8 Hz, 4H, H$^{3,3''}$), 8.77 (m$_c$, 8H, H$^{6,6''}$, H$^{3',5'}$). ^{13}C NMR (CDCl$_3$, 75 MHz, δ): 14.1 (CH$_3$), 22.7, 26.0, 29.2, 29.4, 29.5, 31.8 (CH$_2$), 68.1 (O−CH$_2$), 88.9 (C≡C), 96.5 (C≡C), 114.2, 115.2, 118.7, 121.4, 123.6, 123.9, 127.3, 131.2, 131.6, 132.3, 136.9, 138.6, 142.8, 149.2, 149.3, 156.1, 156.2 (C^{aryl}), 160.3 (C=O). MALDI−TOF MS (dithranol): m/z = 1207.61 (100%, [M + H]$^+$). Anal. Calcd for $C_{80}H_{70}N_8O_2S$: C, 79.57; H, 5.84; N, 9.28; S, 2.66. Found: C, 79.41; H, 5.99; N, 9.08; S, 2.92.

Tetraoctyl 5,5′-([2,1,3]benzothiadiazole-4,7-diylbis(ethyne-2,1-diyl))bis(2-((4-([2,2′:6′,2″]-terpyridine-4′-yl)phenyl)ethynyl)terephthalate) (M6). According to the above-mentioned general procedure, **M6** was obtained after two times column chromatographic purification and three times precipitation from methanol as an orange solid (121 mg, 30%).[51] ^{1}H NMR (CDCl$_3$, 300 MHz, δ): 0.86 (m$_c$, 12H, CH$_3$), 1.19−1.52 (m, 40H, CH$_2$), 1.77−1.89 (m, 8H, OCH$_2$−CH$_2$), 4.40−4.49 (m, 8H, O−CH$_2$), 7.38 (m$_c$, 4H, H$^{5,5''}$), 7.56 (d, ^3J = 8.7 Hz, 4H, H^{a,b}), 7.75 (d, ^3J = 8.4 Hz, 4H, H^{a,b}), 7.95 (m$_c$, 6H, H$^{4,4''}$, H^{C}), 7.97 (d, ^3J = 9.0 Hz, 4H, H^{a,b}), 8.32 (s, 2H, H^{B}), 8.40 (s, 2H, H^{A}), 8.70 (d, ^3J = 7.8 Hz, 4H, H$^{3,3''}$), 8.76 (m$_c$, 4H, H$^{6,6''}$), 8.78 (s, 4H, H$^{3',5'}$). ^{13}C NMR (CDCl$_3$, 75 MHz, δ): 14.1 (CH$_3$), 22.6, 26.1, 28.6, 29.1, 29.2, 29.3, 31.8 (CH$_2$), 66.2 (O−CH$_2$), 88.9 (C≡C), 95.1 (C≡C), 116.0, 118.7, 118.8, 121.4, 123.2, 124.0, 127.3, 127.4, 132.4, 139.0, 139.3, 142.2, 146.9, 149.2, 154.3, (C^{aryl}), 156.0, 156.1 (C=O). MALDI−TOF MS (dithranol): m/z = 1623.85 (100%, [M + H]$^+$). Anal. Calcd for $C_{104}H_{102}N_8O_8S$: C, 76.91%; H, 6.33%; N, 6.90%; S, 1.97%. Found: C, 76.65%; H, 5.98%; N, 6.61%; S 1.80%.

Tetraoctyl 5,5′-(2,5-bis(octyloxy)-1,4-phenylene)bis(ethyne-2,1-diyl)bis(2-((4-([2,2′:6′,2″]-terpyridine-4′-yl)phenyl)ethynyl)terephthalate) (M7). According to the above-mentioned general procedure, **M7** was obtained after two times column chromatographic purification and three times precipitation from methanol as an orange solid (141 mg, 31%).[51] ^{1}H NMR (CDCl$_3$, 300 MHz, δ): 0.82−1.00 (m, 18H, CH$_3$), 1.21−1.65 (m, 60H, CH$_2$), 1.76−1.93 (m, 12H, OCH$_2$−CH$_2$), 3.99−4.09 (m, 4H, O−CH$_2$), 4.34−4.54 (m, 8H, O−CH$_2$), 7.05 (s, 2H, H^{C}), 7.39 (m$_c$, 4H, H$^{5,5''}$), 7.74 (d, ^3J = 8.1 Hz, 4H, H^{a,b}), 7.94 (m$_c$, 6H, H$^{4,4''}$, H^{a,b}), 8.25 (s, 2H, H^{B}), 8.26 (s, 2H, H^{A}), 8.70 (d, ^3J = 7.8 Hz, 4H, H$^{3,3''}$), 8.76 (m$_c$, 4H, H$^{6,6''}$), 8.78 (s, 4H, H$^{3',5'}$). ^{13}C NMR (CDCl$_3$, 75 MHz, δ): 14.1 (CH$_3$), 22.6, 26.1, 28.6, 29.1, 29.2, 29.3, 31.8 (CH$_2$), 66.2 (O−CH$_2$), 88.9 (C≡C), 95.1 (C≡C), 116.0, 118.6, 118. 8, 121.4, 123.2, 124.0, 127.3, 127.4, 132.4, 139.0, 139.3, 142.2, 146.9, 149.2, 154.3, (C^{aryl}), 156.0, 156.1 (C=O). MALDI−TOF MS (dithranol): m/z = 1822.32 (100%, [M + H]$^+$). Anal. Calcd for $C_{120}H_{136}N_6O_{10}$: C, 79.09; H, 7.52; N, 4.61. Found: C, 78.71; H, 7.58; N, 4.32.

General Procedure for the Metallo-Polymerization. To the bis(terpyridine) monomers (**M1**−**M7**, 0.025 mmol) in *N*-methylpyrrolidone (NMP, 5 mL) was added zinc(II) acetate (0.025 mmol) in NMP (1 mL). The resulting solution was stirred at 105 °C under argon atmosphere for 24 h. An excess of NH$_4$PF$_6$ (50 mg) was added to the hot solution and stirring was continued for 1 h. The solution was poured into methanol (50 mL), and the resulting metallo-polymer was filtered off and washed with methanol (10 mL). Further purification was achieved by repeated dissolving of the metallo-polymer in NMP (2 mL) and precipitation from diethyl ether. Finally, the products were dried under vacuum at 40 °C for 24 h.

Metallo-Homo Polymer P1: $\{[\mathrm{Zn}(\mathbf{M1})](\mathrm{PF_6})_2\}_n$. According to the above-mentioned procedure, homo polymer **P1** was obtained as a yellow solid (22 mg, 84%). ^{1}H NMR (DMSO-*d*$_6$, 300 MHz, δ): 7.50 (m$_c$, H$^{5,5''}$), 7.98 (m$_c$, H$^{6,6''}$), 8.32 (m$_c$, H^{aryl}), 8.56 (m$_c$, H$^{4,4''}$), 8.76 (m$_c$, H^{aryl}), 9.17 (m$_c$, H$^{3,3''}$), 9.46 (m$_c$, H$^{3',5'}$). Anal. Calcd for $C_{52}H_{30}F_{12}N_8P_2SZn$: C, 54.11; H, 2.62; N, 9.71; S, 2.78. Found: C, 54.61; H, 2.34; N, 8.98; S, 2.12.

Metallo-Homo Polymer P2: $\{[\mathrm{Zn}(\mathbf{M2})](\mathrm{PF_6})_2\}_n$. According to the above-mentioned procedure, homo polymer **P2** was obtained as yellow solid (29 mg, 82%). ^{1}H NMR (DMSO-*d*$_6$, 300 MHz, δ): 0.72 (m$_c$, CH$_3$), 1.09−1.22 (m, CH$_2$), 4.44 (m$_c$, O−CH$_2$), 7.52 (m$_c$, H$^{5,5''}$), 7.97 (m$_c$, H$^{6,6''}$), 8.30 (m$_c$, H^{aryl}), 8.58 (m$_c$, H$^{4,4''}$), 8.78 (m$_c$, H^{aryl}), 9.18 (m$_c$, H$^{3,3''}$), 9.46 (m$_c$, H$^{3',5'}$). Anal. Calcd for $C_{70}H_{64}F_{12}N_6O_4P_2Zn$: C, 59.69; H, 4.58; N, 5.97. Found: C, 58.91; H, 4.23; N, 4.98.

Metallo-Homo Polymer P3: $\{[\mathrm{Zn}(\mathbf{M3})](\mathrm{PF_6})_2\}_n$. According to the above-mentioned procedure, homo polymer **P3** was obtained as yellow solid (27 mg, 78%). ^{1}H NMR (DMSO-*d*$_6$, 300 MHz, δ): 0.82 (m$_c$, CH$_3$), 1.01 (m$_c$, CH$_3$), 1.18−1.58 (m$_c$, CH$_2$), 3.09 (m$_c$, N=C−CH$_2$), 7.54 (m$_c$, H$^{5,5''}$), 7.99 (m$_c$, H$^{6,6''}$), 8.32 (m$_c$, H^{aryl}), 8.60 (m$_c$, H$^{4,4''}$), 8.79 (m$_c$, H^{aryl}), 9.18 (m$_c$, H$^{3,3''}$), 9.48

Scheme 1. Schematic Representation of the Synthesis of Bis(terpyridines) M1−M7 Using Pd^0-Catalyzed Sonogashira Cross-Coupling Reactions

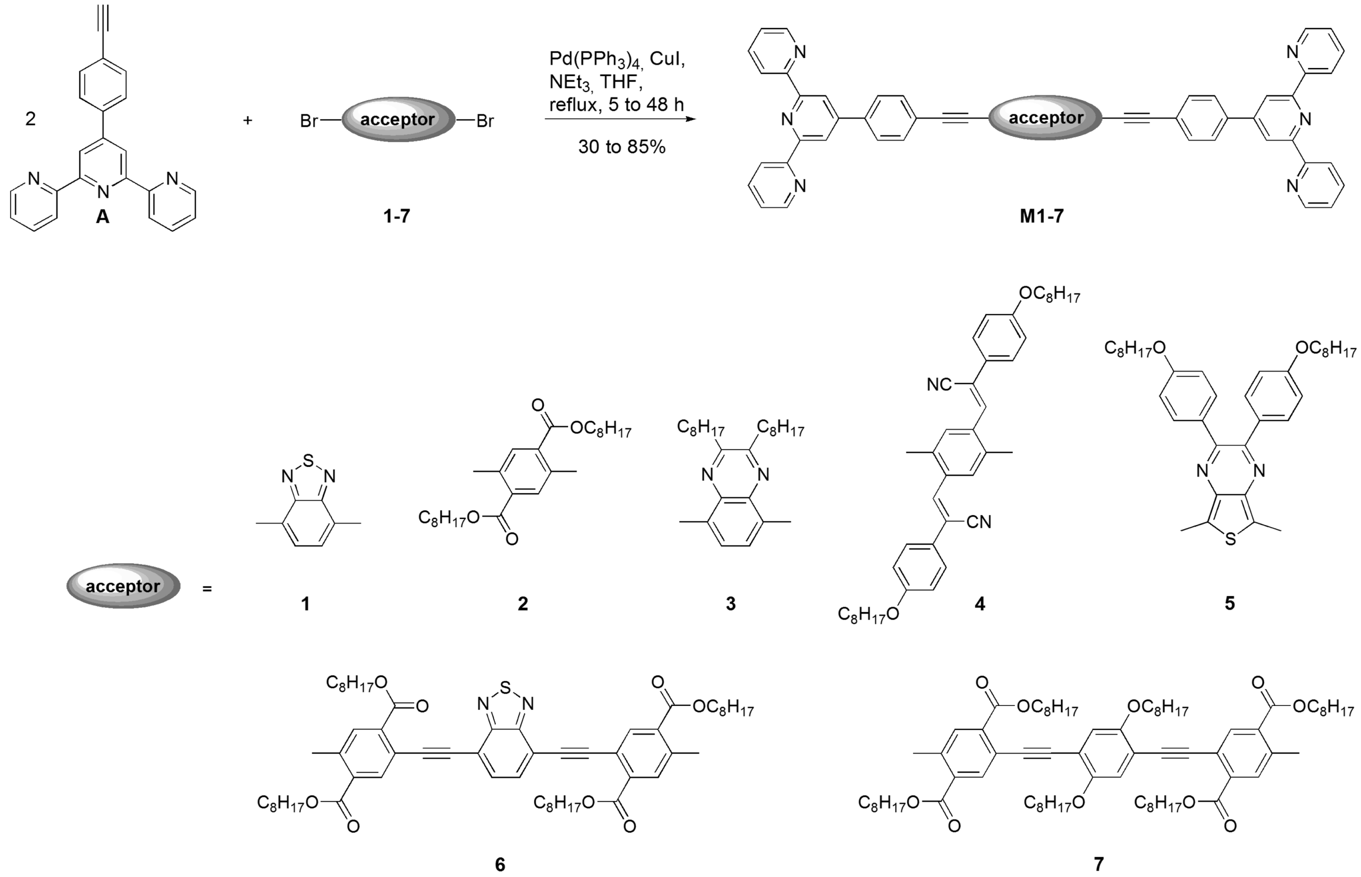

$(m_c, H^{3',5'})$. Anal. Calcd for $C_{70}H_{64}F_{12}N_8P_2Zn$: C, 61.25; H, 4.70; N, 8.16. Found: C, 60.71; H, 4.13; N, 7.58.

Metallo-Homo Polymer P4: $\{[Zn(M4)](PF_6)_2\}_n$. According to the above-mentioned procedure, homo polymer **P4** was obtained after three times precipitation as yellow solid (8 mg, 20%).[51] ^{1}H NMR (DMSO-d_6, 300 MHz, δ): 0.85 (m_c, CH_3), 1.04−1.54 (m, CH_2), 3.08 (m_c, $O-CH_2$), 7.05 (m_c, H^{aryl}), 7.52 (m_c, $H^{5,5''}$), 7.93 (m_c, $H^{6,6''}$), 8.30 (m_c, H^{aryl}), 8.60 (m_c, $H^{4,4''}$), 8.79 (m_c, H^{aryl}), 9.13 (m_c, $H^{3,3''}$), 9.34 (m_c, $H^{3',5'}$). Anal. Calcd for $C_{86}H_{74}F_{12}N_8O_2P_2Zn$: C, 64.28; H, 4.64; N, 6.97. Found: C, 63.78; H, 4.04; N, 6.77.

Metallo-Homo Polymer P5: $\{[Zn(M5)](PF_6)_2\}_n$. According to the above-mentioned procedure, homo polymer **P5** was obtained as orange solid (21 mg, 54%). ^{1}H NMR (DMSO-d_6, 300 MHz, δ): 0.84 (m_c, CH_3), 0.99−1.47 (m, CH_2), 3.99 (m_c, $O-CH_2$), 7.07 (m_c, H^{aryl}), 7.52 (m_c, $H^{5,5''}$), 7.97 (m_c, $H^{6,6''}$), 8.03 (m_c, H^{aryl}), 8.30 (m_c, $H^{4,4''}$), 8.76 (m_c, H^{aryl}), 9.19 (m_c, $H^{3,3''}$), 9.48 (m_c, $H^{3',5'}$). Anal. Calcd for $C_{80}H_{70}F_{12}N_8O_2P_2SZn$: C, 61.48; H, 4.51; N, 7.17; S, 2.05. Found: C, 60.63; H, 3.58; N, 6.64; S, 1.65.

Metallo-homo polymer P6: $\{[Zn(M6)](PF_6)_2\}_n$. According to the above-mentioned procedure, homo polymer **P6** was obtained after three times precipitation as yellow solid (23 mg, 48%).[51] ^{1}H NMR (DMSO-d_6, 300 MHz, δ): 0.75 (m_c, CH_3), 0.98−1.48 (m, CH_2), 4.40 (m_c, $O-CH_2$), 7.52 (m_c, $H^{5,5''}$), 8.06 (m_c, $H^{6,6''}$), 8.08 (m_c, H^{aryl}), 8.30 (m_c, $H^{4,4''}$), 8.68 (m_c, H^{aryl}), 8.77 (m_c, H^{aryl}), 9.15 (m_c, $H^{3,3''}$), 9.41 (m_c, $H^{3',5'}$). Anal. Calcd for $C_{104}H_{102}F_{12}N_8O_8P_2SZn$: C, 63.11; H, 5.19; N, 5.66; S, 1.62. Found: C, 62.47; H, 4.78; N, 5.37; S, 1.22.

Metallo-Homo Polymer P7: $\{[Zn(M7)](PF_6)_2\}_n$. According to the above-mentioned procedure, homo polymer **P7** was obtained as yellow solid (44 mg, 82%). ^{1}H NMR (DMSO-d_6, 300 MHz, δ): 0.76 (m_c, CH_3), 0.97−1.53 (m, CH_2), 4.18 (m_c, $O-CH_2$), 4.40 (m_c, $O-CH_2$), 7.55 (m_c, $H^{5,5''}$), 8.04 (m_c, $H^{6,6''}$), 8.08 (m_c, H^{aryl}), 8.31 (m_c, $H^{4,4''}$), 8.69 (m_c, H^{aryl}), 8.77 (m_c, H^{aryl}), 9.16 (m_c, $H^{3,3''}$), 9.45 (m_c, $H^{3',5'}$). Anal. Calcd for $C_{120}H_{136}F_{12}N_6O_{10}P_2Zn$: C, 66.18; H, 6.29; N, 3.86. Found: C, 65.35; H, 4.23; N, 3.37.

Metallo-Random Copolymer R1: $\{[Zn(M1)](PF_6)_2\}_n\{[Zn(MD1)](PF_6)_2\}_m$. According to the above-mentioned procedure, random copolymer **R1** was obtained as yellow solid (42 mg, 68%). ^{1}H NMR (DMSO-d_6, 300 MHz, δ): 0.90 (m_c, CH_3), 0.99 (m_c, CH_3), 1.26−1.80 (m, CH_2), 4.01 (m_c, $O-CH_2$), 7.56 (m_c, $H^{5,5''}$), 7.78 (m_c, H^{aryl}), 7.99 (m_c, $H^{6,6''}$), 8.13 (m_c, H^{aryl}), 8.32 (m_c, $H^{4,4''}$), 8.58 (m_c, H^{aryl}) 8.74 (m_c, H^{aryl}), 8.78 (m_c, H^{aryl}), 9.15 (m_c, $H^{3,3''}$), 9.41 (m_c, $H^{3',5'}$).

Metallo-Random Copolymer R2: $\{[Zn(M3)](PF_6)_2\}_n\{[Zn(MD2)](PF_6)_2\}_m$. According to the above-mentioned procedure, random copolymer **R2** was obtained as green-yellow solid (48 mg, 70%). ^{1}H NMR (DMSO-d_6, 300 MHz, δ): 0.80 (m_c, CH_3), 0.94−1.57 (m_c, CH_2), 3.14 (m_c, $O-CH_2$), 7.54 (m_c, $H^{5,5''}$), 7.66 (m_c, H^{aryl}), 7.78 (m_c, H^{aryl}), 7.99 (m_c, $H^{6,6''}$), 8.06 (m_c, H^{aryl}), 8.31 (m_c, $H^{4,4''}$), 8.58 (m_c, H^{aryl}), 8.69 (m_c, H^{aryl}), 8.77 (m_c, H^{aryl}), 9.18 (m_c, $H^{3,3''}$), 9.47 (m_c, $H^{3',5'}$).

Results and Discussion

Synthesis and Characterization of Monomers M1−M7. The synthetic route towards the ditopic bis(terpyridine) monomers **M1−M7** is illustrated in Scheme 1. The acceptor-type spacer units (**1−7**) were synthesized in multistep procedures, starting from commercial available compounds (see the Supporting Information for details). According to Scheme 1, the aromatic dibromides **1−7** were reacted with two equivalents of 4′-(4-ethynylphenyl)-[2,2′:6′,2″]terpyridine (**A**) under Pd^0-catalyzed Sonogashira cross-coupling conditions. After precipitation from methanol and column chromatographic purification, the bis(terpyridines)

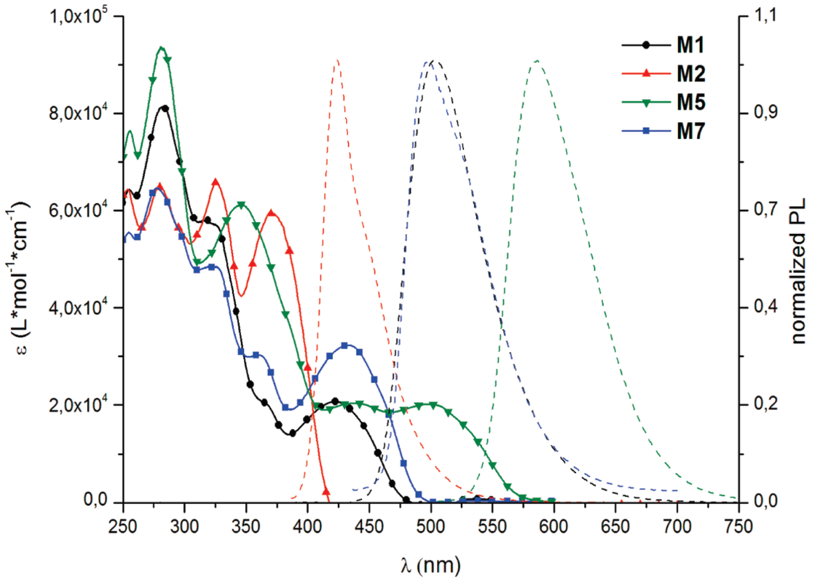

Figure 1. UV−vis absorption (solid lines) and normalized photoluminescence spectra (dashed line) of selected bis(terpyridines). For all spectra: 10^{-6} M in CHCl$_3$, room temperature.

Table 1. Selected Photophysical Properties of Bis(terpyridines) M1−M7

bis(terpyridine)	$\lambda_{\mathrm{abs,max}}$[a] (nm)	$\lambda_{\mathrm{PL,max}}$[a] (nm)	$\varepsilon \times 10^4$[a,b] (M^{-1}·cm^{-1})	Φ_{PL}[a,c]	Stokes shift (cm^{-1})	E_g^{opt}[d] (eV)
M1	423, 365, 316, 282	503	2.07	0.79	3760	2.62
M2	373, 325, 279, 254	424	5.93	0.63	3225	3.00
M3	395, 317, 267, 252	443	3.01	0.68	2743	2.83
M4	401(s), 354, 283, 253	484, 509(s)	8.80	0.37	4277	2.74
M5	498, 440, 346, 281, 255	587	2.02	0.69	3045	2.17
M6	433, 361, 322, 279, 255	498	3.23	0.65	3014	2.58
M7	427, 361, 328, 283	490	2.39	0.57	3011	2.56

[a] For all spectra: 10^{-6} M in chloroform; (s) = shoulder. [b] Extinction coefficients of the lowest-energy absorption band. [c] Absolute quantum yields, uncorrected with respect to reabsorption. [d] $E_g^{opt} = h \cdot c/\lambda_{0.1\mathrm{max}}$.

M1−**M7** were obtained in moderate to good yields and fully characterized by NMR, UV−vis absorption, and photoluminescence spectroscopy as well as MALDI−TOF mass spectrometry and elemental analysis. The photophysical properties of **M1**−**M7** are summarized in Figure 1 and Table 1.

In order to investigate the influence of the electron-acceptor spacers and the length of the π-conjugated system on the photophysical properties of bis(terpyridines) **M1**−**M7**, UV−vis absorption and photoluminescence spectra were measured. In accordance with the literature, the absorption spectra of the ditopic ligands **M1**−**M7** featured two intense band regions.[2,9,10,32,33,52] The bands at about 250 to 350 nm were assigned to the characteristic π−π* transitions of the terpyridine moieties and show high extinction coefficients (ε) up to 95,000 M^{-1}·cm^{-1}.[23,28,33,52] Furthermore, the spectra are characterized by an intensive band in the visible region (λ_{abs} = 370−498 nm) corresponding to π−π* transitions of the overall π-conjugated system with extinction coefficients up to 88 000 M^{-1}·cm^{-1}. However, in comparison to all other synthesized systems, bis(terpyridine) **M5** showed the most pronounced bathochromic shift of the absorption maximum and, thereby, the smallest optical energy band gap, although **M5** bears *n*-octyl chains which are known to disturbe rigidity and planarity.[48] This indicates a strong electronic interaction of the lateral electron-rich *p*-dialkoxy-benzene substituents with the electron-poor thieno[3,4-*b*]pyrazine unit, resulting in a push−pull effect. In consequence of this interaction, the quinoide contribution to the electronic structure of the ground state is increased, resulting in a destabilization of the HOMO energy location with a simultaneous stabilization of the LUMO energy location, which induces a significantly lowered energy band gap and a strong red-shift of the absorption, as observed. The dimension of this bathochromic shift correlates well with the intensity of the intramolecular charge transfer.[34] The π-extended systems **M6** and **M7** also exhibit a bathochromic shift as well as a lowered energy band gap, in comparison to their analogues with smaller spacer units (**M1** and **M2**). In particular, the comparison of **M6** and **M1** reveals that the influence of the π-extension is partially compensated by a steric hindrance due to the alkyl chains, which results only in a small red-shift of the absorption maximum of about 10 nm. The increase of the extinction coefficient of **M6** relative to **M1** can be ascribed to an increasing absorption cross section of the central chromophores within the bis(terpyridines).[33]

The photoluminescence spectra and absolute quantum yields were obtained by excitation at the lowest-energy absorption maxima of the bis(terpyridine) systems. In dilute solution, emission maxima in the range of 392 to 587 nm, corresponding to Stokes shifts between 2700 and 4500 cm^{-1}, were observed. The large Stokes shift of bis(terpyridine) **M4** (4300 cm^{-1}) can be explained by a more extended conjugation in the excited state in comparison to the other systems.[33,50] Theoretical calculations on these systems would help to investigate this behavior further.

In general, the photoluminescence properties are equally influenced by the electronic structure as previously discussed for the UV−vis absorption behavior. Again, bis(terpyridine) **M5** showed the most distinctive bathochromic shift of the

Scheme 2. Schematic Representation of the Metallo-Polymerization of M1−M7 to the Homo Polymers P1−P7 (Top) and Random Copolymers R1 and R2 (Bottom)

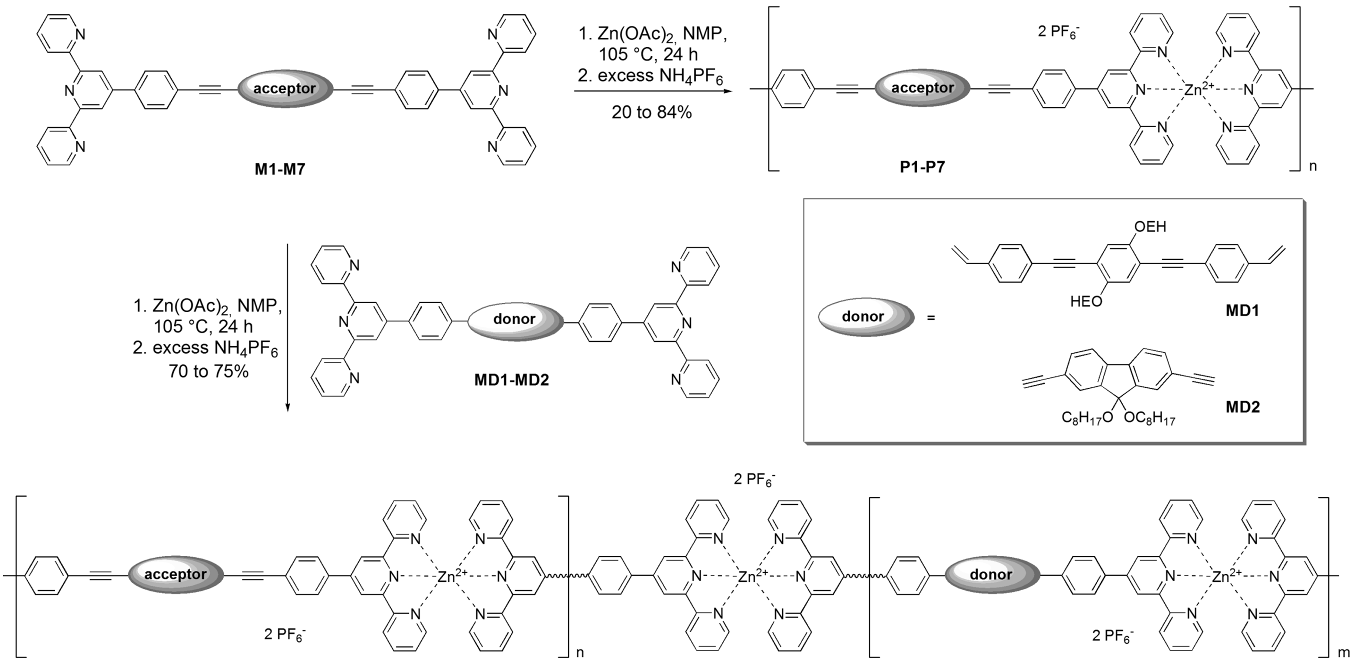

R1: $\{[Zn(\mathbf{M1})](PF_6)_2\}_n\{[Zn(\mathbf{MD1})](PF_6)_2\}_m$

R2: $\{[Zn(\mathbf{M3})](PF_6)_2\}_n\{[Zn(\mathbf{MD2})](PF_6)_2\}_m$

emission maximum, thus the effects mentioned above have to be considered again. As a consequence of its Stokes shift (3000 cm^{-1}), **M5** emits with an intensive orange-red color ($\lambda_{PL,max}$ = 587 nm).

By incorporation of electron-rich dialkoxy-benzene subunits into the spacer (push−pull effect) and the resulting elongation of the π-conjugation, the emission maximum of **M7** (bright green emission) is notably red-shifted in comparison to the structurally related bis(terpyridine) **M2** (blue emission).

All ditopic ligands featured high quantum yields (Φ_{PL}) in the range of 40 to 80%. The highest quantum yields were obtained for bis(terpyridines) **M1** and **M5**.

Synthesis of the Zinc(II)-Containing Metallo-Polymers. The synthesis of the Zn^{II}-based metallo-polymers is depicted in Scheme 2. The metallo-polymerization by self-assembly was carried out according to methods described in literature.[9,16,23] Bis(terpyridines) **M1−M7** were heated with zinc(II) acetate at an exact stoichiometric ratio of 1:1 in *N*-methylpyrrolidone (NMP), followed by subsequent anion exchange with ammonium hexafluorophosphate to yield the metallo-homo polymers **P1−P7**. In the case of the random copolymers (**R1** and **R2**) donor-type bis(terpyridines)[50] with a dialkoxy-benzene (**MD1**) and a fluorene spacer unit (**MD2**), respectively, were utilized in combination with the acceptor-type bis(terpyridines) (**M1** and **M3**). Here, both ditopic ligands were used in a 1:1 ratio in order to obtain metallo-copolymers with a 50% content of each monomer. Since, no signals are separated in the NMR spectra of **R1** and **R2**, we could not apply a selective integration in order to get information about the arrangement of the monomers (alternating/random) along the polymer chains. For this purpose, we assume a random distribution in both copolymers (**R1** and **R2**).

The resulting polymers were purified by repeated precipitation from NMP in diethyl ether and dried in vacuum, leading to homo polymers **P1−P7** (yield: 20−84%) and random copolymers **R1** and **R2** (yields: 75% and 70%, respectively). Because of the reactivity of Zn^{II} ions and the stability of the bis(terpyridine)−Zn^{II} moieties, the self-assembly process occurs under comparably mild conditions.[23,24]

In comparison to the monomers **M2−M7** (**M1** was hardly soluble itself), all metallo-polymers showed a significantly decreased solubility in common organic solvents. This behavior is mainly caused by the highly linear-rigid structure of the polymer backbone as well as by the involved charged metal ions attached leading to solubility only in highly polar aprotic solvents, e.g., DMSO, DMF, NMP, or acetonitrile.[9,23,24]

The molar mass of the resulting polymers could not yet be determined because both size exclusion chromatography (SEC) and MALDI−TOF mass spectrometry were not usable for the characterization of Zn^{II}-based metallo-polymers. In contrast to related ruthenium(II)- or nickel(II)-containing metallo-polymers,[53] Zn^{II}-based systems are not stable under the measurement conditions owing to a considerably weaker binding strength of the terpyridine ligand to the metal ion.[2]

However, characterization by ^{1}H NMR spectroscopy indicated the formation of the desired metallo-polymers by broadened signals of the terpyridine ligand, which is a typically feature of polymeric materials, as well as by the absence of the signals from the uncomplexed terpyridine unit (Figure 2). Additionally, this behavior proves that the polymeric structure remains unaffected in polar solvents. Furthermore, and in accordance with the literature, a clear downfield shift of the (5,5″)-, (4,4″)-, (3,3″)- and (3′,5′)-terpyridine signals, upon coordination to the Zn^{II} ions, was observed.[9,19,23,24] The (6,6″)-terpyridine signals are significantly upfield shifted due to the location above the ring plane of the adjacent ligand. These assignments are based on the comparison of the spectra to those reported for related homoleptic Zn^{II} model complexes.[9,24] A calculation of the molar mass of the metallo-polymers via the integration of end group-signals was not possible due to the absence of any end group-signals. However, considering the typical limit of the NMR spectroscopy (≈ 5%), the synthesized metallo-polymers should consist of more than 30 repeating units [for comparison, see ref 60]. Hence, the molar mass of **P1**−**P7** was estimated to be not less than 25 000 to 50 000 g/mol.

Additionally, elemental analysis of the obtained metallo-polymers provides an indication that the relative composition is close to the expected stoichiometric ratio of 1:1 for the Zn^{II} ions and bis(terpyridine) ligands.

For further characterization of the homo polymers **P1**−**P7**, UV−vis titration experiments were carried out to confirm their supramolecular structure (Figure 3). It is known from the literature that the formation of linear metallo-polymers can be controlled by the exact stoichiometric ratio of metal ion to ditopic ligand.[9,24,28] Upon stepwise addition of Fe^{II} to a solution of bis(terpyridine) **M2**, the absorption spectra revealed the appearance of a metal-to-ligand charge-transfer (MLCT) band at 583 nm, characteristic for iron(II)-based supramolecular assemblies. Furthermore, a shift of three other absorption bands at 373, 333, and 260 nm could be observed. The intensity of the MLCT band is increasing linearly up to a stoichiometric ratio of 1:1, which indicates the formation of a metallo-polymer.

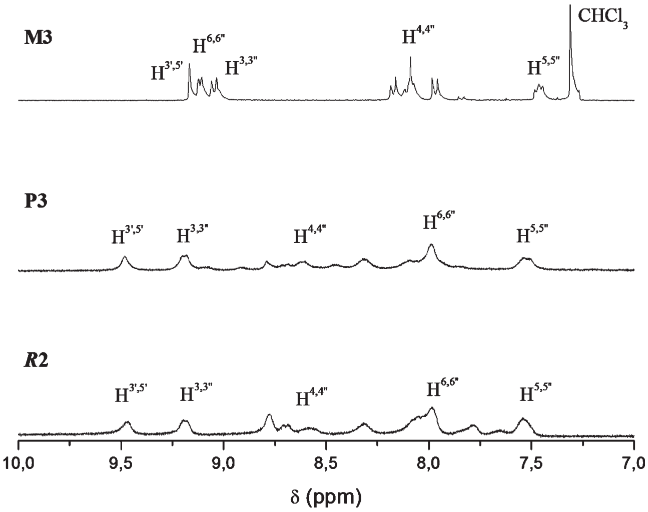

Figure 2. ^1H NMR spectra (aromatic region) of bis(terpyridine) **M3** (top, $CDCl_3$), homo polymer **P3** (middle, DMSO-d_6) and random copolymer **R2** (bottom, DMSO-d_6). The signals belonging to the terpyridine moiety are assigned; the other signals correspond to the π-conjugated spacer. For all spectra: 300 MHz, room temperature.

The absence of any shoulder at the $\pi-\pi^*$ transition of the whole π-conjugated system at 373 nm with increasing addition of Fe^{II} ions accommodates to the fact that an electron-withdrawing spacer unit is attached to the terpyridine. Usually this circumstance is attributed to a charge-transfer occurring between electron-rich spacer units and the electron deficient metal-coordinated terpyridine moiety.[23,28]

The titration experiments clearly revealed that at a 1:1 ratio of metal ion to bis(terpyridine) ligand a supramolecular assembly is formed. Depolymerization beyond the point of equivalence[23,24] has not been observed in the present case due to the stable $Fe^{II}(tpy)_2$ moiety.

Electrochemical Properties. Applying cyclic voltammetry, the energy levels of the HOMO, corresponding to the ionization potential, and of the LUMO, corresponding to the electron affinity, can be estimated. The electrochemical properties of the homo polymers (**P1**−**P7**) and random copolymers (**R1** and **R2**) were obtained from thin films of the materials coated on Pt wires and are summarized in Table 2 and Figure 4.

All homo polymers (**P1**−**P7**) and both random copolymers (**R1** and **R2**) exhibited quasi-reversible reduction peaks between −1.29 and −1.65 V at scans up to −2.5 V. In agreement with the literature, these waves were attributed to the reduction of the terpyridine moiety and the attached π-conjugated spacer unit inside the polymers.[23,24,28] Furthermore, most of the metallo-polymers featured distinct reduction waves at more negative potentials. As expected, no significant oxidation processes were observed up to 1.5 V. Because of the stable d^{10} electron configuration of the Zn^{II} metal centers, oxidation is difficult to observe.[23,24,28] The estimated LUMO levels are based on the first reduction wave

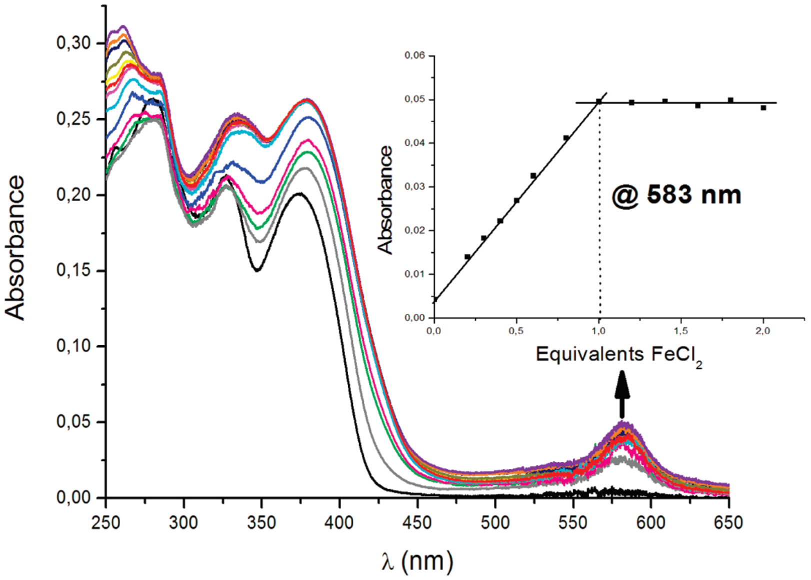

Figure 3. UV−vis absorption spectra acquired upon the titration of monomer **M2** (10^{-5} M in chloroform) with $FeCl_2$ (10^{-4} M in methanol). The absorption at the MLCT band (583 nm) as a function of added $FeCl_2$ solution is shown as an inset.

Table 2. Electrochemical Properties of the Homo Polymers P1−P7 and the Random Copolymers R1 and R2, respectively

polymer	$E_{1/2}^{red\,a}$ (V)	$E_{onset}^{red\,a}$ (V)	LUMO[b] (eV)	HOMO[c] (eV)	$E_g^{opt\,d}$ (eV)
P1	−1.44, −1.81, −2.05	−1.69	−3.16	−5.75	2.59
P2	−1.29, −1.60	−1.49	−3.36	−6.21	2.85
P3	−1.29, −1.62	−1.49	−3.36	−6.14	2.78
P4	−1.61, −2.16	−1.68	−3.17	−5.90	2.73
P5	−1.65, −2.19	−1.63	−3.22	−5.30	2.08
P6	−1.61, −2.01	−1.62	−3.23	−5.56	2.33
P7	−1.65	−1.45	−3.40	−5.91	2.51
R1	−1.54, −1.87	−1.73	−3.12	−5.88	2.76
R2	−1.29, −1.66, −1.95	−1.54	−3.31	−6.22	2.91

[a] Half-wave potential of the reduction waves (films (0.1 M (TBA)PF_6 in CH_3CN) coated on Pt wires, scan rate 50 mV·s^{-1}); potentials are reported versus a Ag/Ag^I electrode (Ag in 0.1 M $AgNO_3$ solution). [b] LUMO levels were calculated from the measured first reduction potential versus Fc/Fc^+ according to eq 1. [c] HOMO levels were calculated from the optical band gap E_g^{opt} and the respective LUMO levels. [d] $E_g^{opt} = h \cdot c/\lambda_{0.1\max}$.

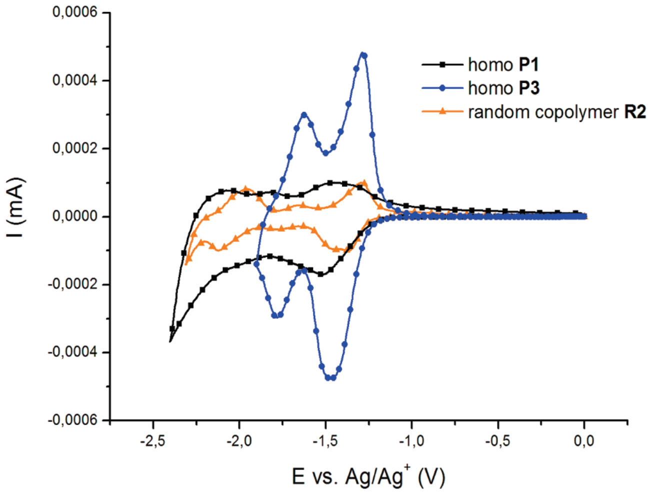

Figure 4. Cyclic voltammograms of selected metallo-polymers (cathodic scans are shown). For all measurements: films (0.1 M (TBA)PF_6 in CH_3CN,) coated on Pt wires, scan rate 50 mV/s.

and on the reference energy level of ferrocene, according to eq 1.[54]

$$E^{\mathrm{LUMO}} = [-(E_{onset}^{red} - E_{onset}^{reference}) - 4.8]\ \mathrm{eV} \qquad (1)$$

The LUMO levels range between −3.12 and −3.40 eV. Since no oxidation potentials could be determined, the corresponding estimation of the ionization potential (i.e., the HOMO energy level) and the electrochemical band gap could not be derived. Therefore, the optical energy band gaps of the metallo-polymers were estimated from the UV−vis absorption spectra by extrapolating to the 0−0 transition of the longest wavelength absorption band (at 10% of the absorption maximum). They ranged from 2.08 to 2.85 eV and were strongly influenced by the nature of the attached π-conjugated spacer unit. In order to obtain any information about the HOMO levels of the Zn^{II} metallo-polymers, the calculated optical band gaps E_g^{opt} and LUMO levels were used for the estimation. HOMO levels from −5.30 to −6.22 eV were derived. Taking this into account, the photophysical and electrochemical properties of the metallo-polymers can be tuned by variation of the chromophore, which was shown representatively for the small energy band gap of homo polymer **P5**.

Photophysical Properties. Further investigation on the photophysical properties of homo polymers **P1**−**P7** and, in particular, of the random copolymers **R1** and **R2**, was carried out by UV−vis absorption and photoluminescence spectroscopy. The spectroscopic data are summarized in Table 3 and Figures 5−7. In general, all metallo-polymers showed − in agreement with the observations for the bis(terpyridines) **M1**−**M7** — characteristic absorptions between 250 and 480 nm, where the transitions at higher energy correspond to the terpyridine motive itself and the lower energy transitions to absorptions of the whole π-conjugated system. As expected, the Zn^{II} cores do not participate in the transitions, due to the filled d^{10} electron shell. Furthermore, a mostly hypsochromic shift of the π−π* transition of 5 to 25 nm compared to the free bis(terpyridines) was observed. As reported for Zn^{II}-based metallo-polymers with electron-donating spacer units, a charge-transfer (CT) between electron-rich central units and the metal-coordinated electron-deficient terpyridine unit causes a red-shift in absorption.[55] In the present cases, the central chromophores consist of electron-withdrawing groups which are not able to undergo such CT processes with the terpyridine units. Inductive effects, which are caused by the complexed metal ion, do not compensate the missing CT and, therefore, result in a small blue-shift of the absorption bands. Additionally, the UV−vis absorption data of the metallo-polymers revealed a considerable decrease of the values of the extinction coefficients (Tables 1 and 2), which might be caused by a parallel arrangement of the dipole moments of the bis(terpyridine) units within the polymer backbone.[24]

Homo polymer **P5** resembled this behavior impressively with a decrease in the extinction coefficient of about one order of magnitude. It simultaneously exhibits the highest absorption wavelength (λ_{abs} = 485 nm) and, therefore, the smallest distance between the HOMO and the LUMO energy level. On the other hand, homo polymer **P2** possesses the lowest absorption wavelength (λ_{abs} = 362 nm), equivalent with the largest HOMO−LUMO energy band gap. The values for E_g^{opt} were obtained by extrapolating the tails of the lowest energy absorption edge to the 0−0 transition as mentioned above.

The homo polymers (**P1**−**P7**) covered a wide range of PL emission maxima from 424 to 586 nm (Figure 5, dashed line), which strongly depends on the effective π-conjugation length and push−pull effects in the case of homo polymer **P5** (see above). Also absolute photoluminescence quantum yields (Φ_{PL}) of the materials were determined. In the case of the homo polymers, a decrease of Φ_{PL} in comparison to the ditopic terpyridine ligands **M1**−**M7** upon complexation was observed (**M1**−**M7**, Φ_{PL} = 0.37−0.79; **P1**−**P7**, Φ_{PL} = 0.18−0.66). Whereas **P7** showed only a third of the value measured for the corresponding bis(terpyridine) **M7**, only a small decrease of 15% was detected for **P3** relative to **M3**.

In comparison to conventional π-conjugated polymers bearing similar backbone units, the metallo-polymers exhibited higher PL quantum yields. The group of Klemm obtained for similar thieno[3,4-*b*]pyrazine-bearing π-conjugated polymers Φ_{PL} values in solution of about 0.15, which correlates with a 3-fold larger value for **P5**.[49,56] In addition,

Table 3. Selected Photophysical Properties of the Homo Polymers P1−P7 and the Random Copolymers R1 and R2, respectively

polymer	$\lambda_{\text{abs,max}}{}^{a}$ (nm)	$\lambda_{\text{PL,max}}{}^{a}$ (nm)	$\varepsilon \times 10^{4\,a,b}$ ($M^{-1}\cdot cm^{-1}$)	$\Phi_{\text{PL}}{}^{a,c}$	Stokes shift (cm^{-1})	$E_g{}^{opt\ d}$ (eV)
P1	415, 359, 321, 284	513	0.99	0.66	4603	2.59
P2	362, 325, 279	424	2.74	0.43	4039	2.85
P3	392, 322, 288	443	1.75	0.53	2937	2.78
P4	397 (s), 362, 331, 284	446	2.35	0.26	2767	2.73
P5	485 (s), 400 324 (s), 288	586	0.33	0.42	3554	2.08
P6	405, 317, 284	511	2.69	0.31	5122	2.33
P7	411, 326, 284	518	2.24	0.18	5026	2.51
R1	404, 337, 284	453, 470 (s)	9.07	0.90	2677	2.76
R2	369, 320, 281	409 (s), 432	11.25	0.81	3952	2.91

[a] For all spectra: 10^{-6} M in DMF; (s) = shoulder. [b] Extinction coefficients at the lowest-energy absorption band. [c] Absolute quantum yields, uncorrected with respect to reabsorption. [d] $E_g{}^{opt} = hc/\lambda_{0.1\text{max}}$.

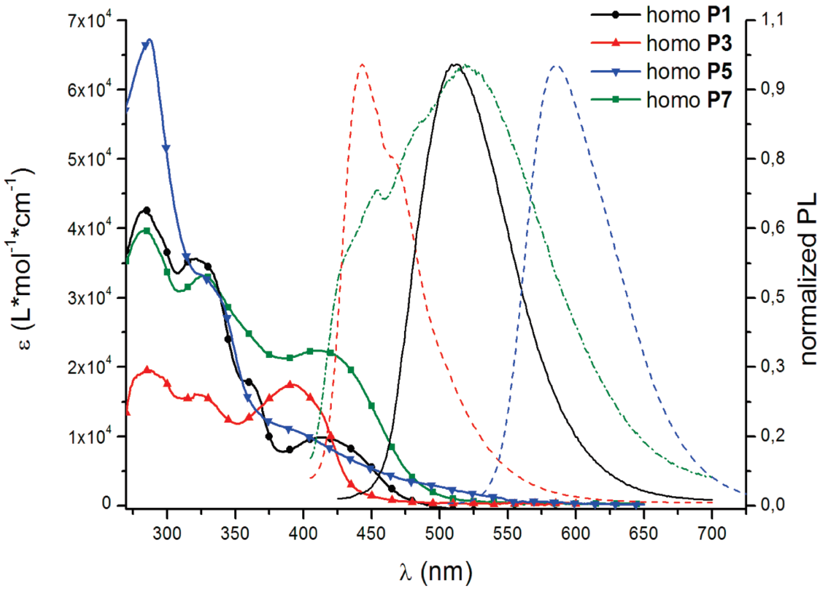

Figure 5. UV−vis absorption (solid line) and normalized photoluminescence spectra (dashed line) of selected homo polymers. For all spectra: 10^{-6} M in DMF, room temperature.

Chen et al. reported Φ_{PL} values of [2,1,3]benzothiadiazole- and quinoxaline-bearing π-conjugated polymers of about 0.19 and 0.22, respectively.[57] Compared to these π-conjugated polymers, metallo-polymers **P1** and **P3** (Φ_{PL} = 0.66 to 0.53) emit much more efficiently.

Moreover, the random copolymers **R1** and **R2** were characterized by UV−vis absorption and PL spectroscopy in order to study the influence of a donor- and acceptor-bridged bis(terpyridine) within one Zn^{II} metallo-polymer (Figures 6 and 7).

Therefore, the UV−vis absorption spectra of the individual donor- and acceptor-based homo polymers (**P8**[58] and **P1**, respectively) were compared to that of random copolymer **R1** (Figure 6, top). Additionally, the spectra of both homo polymers were numerically summed up. The resulting spectrum showed good conformity of the appearing bands with the experimental spectrum of **R1**, but less accordance with the measured extinction coefficients. The latter fact might be a hint for a deviation from the exact 1:1 ratio of the monomeric bis(terpyridines) (**M1** and **MD1**) within the present random copolymer **R1**, attributed to a small excess of the **MD1**. The overall UV−vis absorption spectrum of **R1** is dominated by three bands between 250 to 420 nm, corresponding to the aforementioned characteristic transitions. Because of the large difference in the extinction coefficient between donor-type (**P8**) and acceptor-type homo polymer (**P1**) ($\varepsilon = 5.3 \times 10^4\ M^{-1}\cdot cm^{-1}$ and $\varepsilon = 0.99 \times 10^4\ M^{-1}\cdot cm^{-1}$, respectively), the extinction of the $\pi-\pi^*$ transition of the random copolymer **R1** is predominated by the donor-part. The same applies also for the PL emission of **R1**. Excitation at the lowest energy absorption band of random copolymer **R1** (λ_{ex} = 404 nm) prefers considerably the PL emission of the electron-donating part. By means of variegating the excitation wavelengths to smaller extinction differences, e.g., λ_{ex} = 440 nm (Figure 6, bottom), and by measuring the PL emission of different molar ratios of the ditopic monomers (**MD1** and **M1**, see Figure 6, middle left), the emission behavior of the random copolymer **R1** could be attributed mainly to the large extinction coefficient. At wavelengths with almost equivalent extinction coefficients (e.g., λ_{abs} = 440 nm) the PL emission of the acceptor is dominating. This leads to the assumption that the very high quantum yield of **R1** (Φ_{PL} = 0.90) is caused by both parts and that an energy transfer from the donor to the acceptor moiety within the random copolymer **R1** is not favored.

Consequently, a second donor−acceptor pair was chosen for random copolymer **R2**, which exhibits a preferably large overlap of acceptor absorption with the emission of the donor unit, in order to achieve similar energies for several vibronic transitions of the donor and the acceptor, leading to a resonant coupling. These are requirements to obtain an energy transfer, in particular of the Förster-type (FRET).[36,37] From the materials at hand, the acceptor-based bis(terpyridine) **M3** with a quinoxaline spacer-unit and a donor-based bis(terpyridine) bearing a fluorene-moiety (**MD2**,[58] see Scheme 2) provide these conditions. The position of the

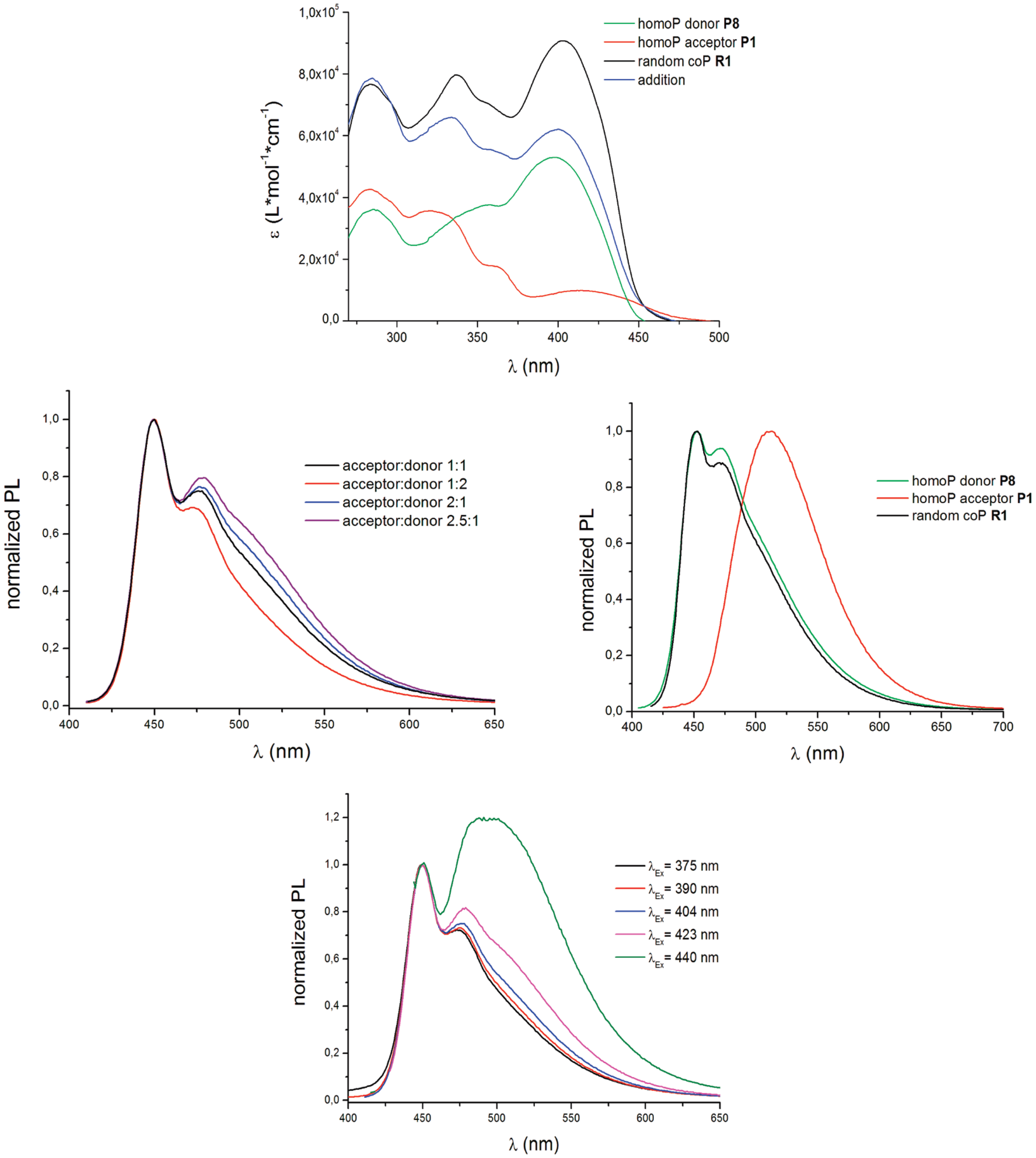

Figure 6. Top: UV−vis absorption spectra of random copolymer **R1** compared to the homo polymers of the acceptor-based bis(terpyridine) (**P1**) and the donor-based bis(terpyridine) (**P8**).[58] Middle left: Normalized PL spectra obtained at different acceptor (**M1**) to donor (**MD1**) ratios. Middle right: Normalized PL spectra of **R1** compared to the homo polymers of the acceptor-based (**P1**) and the donor-based bis(terpyridine) (**P8**). Bottom: Normalized PL spectra of **R1** at different excitation wavelengths. For all spectra: (10^{-6} M in DMF).

PL emission maximum of the donor bis(terpyridine) (λ_{PL} = 403 nm) is almost at the same wavelength as the $\pi-\pi^*$ transition of the π-conjugated system of the acceptor **M3** (λ_{abs} = 396 nm). Additionally, the extinction coefficients are in a comparable order of magnitude.

Therefore, the UV−vis absorption spectra of both monomers were measured and numerically added (Figure 7, top). The resulting spectrum is almost identical to the measured UV−vis absorption spectrum of random copolymer **R2**, both in band positions and in the extinction coefficients. This is an indication for an almost 1:1 ratio of the donor and acceptor within the synthesized copolymer. As for **R1**, the typical $\pi-\pi^*$ transitions of the terpyridine and the whole π-conjugated system were obtained for **R2**. The longest

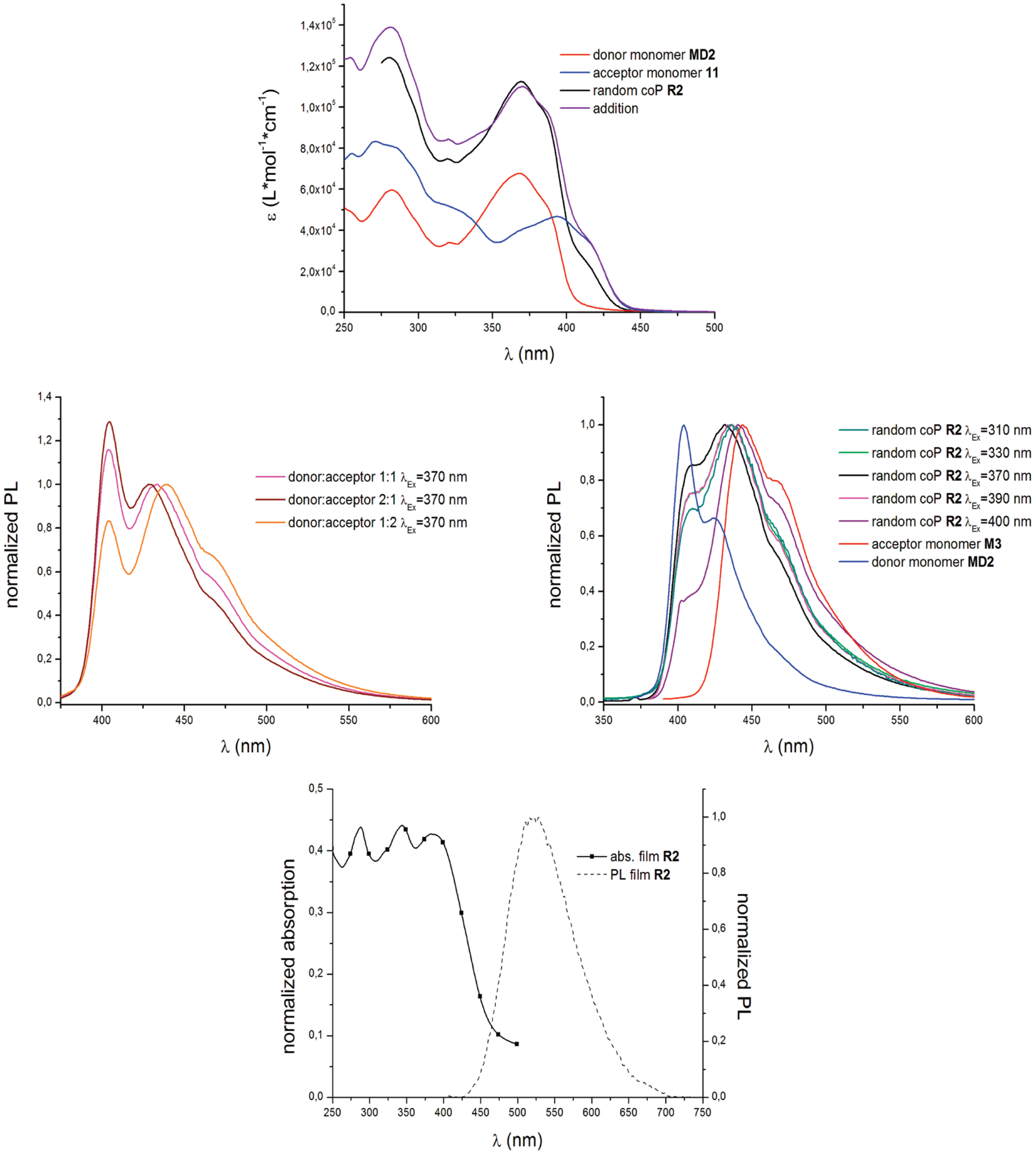

Figure 7. Top: UV−vis absorption spectra of **R2** compared to the acceptor-based bis(terpyridine) (**M3**) and the donor-based bis(terpyridine) (**MD2**).[58] Middle left: Normalized PL spectra obtained at different acceptor (**M3**) to donor (**MD2**) ratios. Middle right: Normalized PL spectra of **R2** at different excitation wavelengths compared to the monomers **M3** and **MD2**. Bottom: UV−vis absorption and photoluminescence (PL) spectra of random copolymer **R2** in the solid state (80 nm thickness). For all spectra: 10^{-6} M in DMF, respectively, spin coated from DMF solution (20 mg/mL, 1000 rpm, 100 s).

wavelength absorption band of random copolymer **R2** is located at 370 nm with a shoulder at 411 nm, induced by the long wavelength flank of the acceptor system.

In order to gain further insight into the behavior of random copolymer **R2** at the excited state, the PL properties were investigated. In a first experiment the donor- and acceptor-monomers (**MD2** and **M3**) were mixed in different molar ratios (Figure 7, middle left) and excited at their longest wavelength absorption maximum. At a 1:1 ratio the emission originating from the donor bis(terpyridine) (**MD2**) is slightly dominating due to the larger extinction coefficient at 370 nm, which inverses with increasing acceptor portion. Consequently, the PL behavior of the mixtures of **MD2** and **M3** is only an addition of both monomers and no energy transfer was observed. Nevertheless, excitation at the longest absorption band wavelength of the random copolymer **R2** resulted in a completely different PL emission spectrum (Figure 7, middle right). In this case, the emission attributed to the acceptor-unit, though slightly red-shifted, was clearly dominating. Only a shoulder confirms the emission originating from the donor-part. Both, decreasing as well as increasing the excitation wavelength, lead to a further reduction of the donor-based emission. At λ_{ex} = 370 nm the emission ratio of the acceptor- to the donor-unit is 1:0.85, although the ratio of the extinction coefficients at this particular wavelength (1:1.66) indicates a larger absorption of the donor.

This circumstance can be explained by a radiationless transfer of energy from the excited donor moieties in random copolymer **R2** to the electron-accepting units.[36,37,59] This leads to the excitation of the acceptor-parts, which are now able to deactivate under emission of the transferred energy.[36] The fact that a simple mixture of the involved monomers (**MD2** and **M3**) revealed no indication for an energy transfer whereas the corresponding Zn^{II}-based random copolymer is able to do, shows that the central Zn^{II}–terpyridine moieties play a crucial role for the mediation of such a transfer.

In order to obtain information about the applicability of Zn^{II} metallo-polymers as OLED devices, the solid-state properties are crucial. Therefore, the photophyiscal properties of random copolymer **R2** in the solid state were additionally investigated. Low solubility of all synthesized metallo-polymers in common organic solvents was observed. Spin-coating from DMF solution (20 mg/mL, 1000 rpm, 100 s) was applied, resulting in a homogeneous film (80 nm thickness) of random copolymer **R2** which was used for the UV–vis absorption and photoluminescence measurements (Figure 7, bottom). The spectra reveal a slight hypsochromic shift (10 nm) of the absorption maximum in comparison to those observed in solution. However, the PL maximum shows a bathochromic shift of 90 nm in comparison to the solution of random copolymer **R2**. In accordance with the literature, this large Stokes shift of about 7000 cm^{-1} can be attributed to strong intermolecular π–π-interactions of the metallo-polymeric chains. This behavior results from a very close orientation in the solid state, which prefers a disturbance among themselves and destabilizes occupied orbitals.[24,28,30]

Conclusion

In summary, a logical synthesis route for a set of π-conjugated bis(terpyridine) ligands bearing electron-withdrawing spacer units and their corresponding main chain metallo-homo polymers was developed. The formation of the metallo-polymers was concluded from the broadened ^{1}H NMR signals as well as from UV–vis titration experiments. ^{1}H NMR provides an estimation of the molar mass of approximately 25 000–50 000 g/mol. Apparently, the electro-optical properties of the monomers as well as of the homo polymers are strongly influenced by the nature of the attached π-conjugated spacer unit and shows some distinct differences in comparison to related electron-donating Zn^{II} metallo-polymers. Furthermore, two donor–acceptor random copolymers were synthesized and their electro-optical properties were investigated by UV–vis absorption as well as PL spectroscopy. Thereby, random copolymer **R2** featured an energy transfer from the donor to the acceptor unit, which was confirmed by various emission experiments in solution. The central role of the Zn^{II}–terpyridine moiety within the materials was concluded from these results. Furthermore, the solid-state properties of random copolymer **R2** were investigated in order to obtain information about the potential applicability of Zn^{II} metallo-polymers as OLED devices.

The herein synthesized metallo-polymers (homo and random) show promising properties with respect to potential opto-electronic applications in OLED or PLED devices.

Acknowledgment. The authors acknowledge the financial support from the Dutch Polymer Institute (DPI), the Nederlandse Organisatie voor Wetenschappelijk Onderzoek (NWO, VICI award for U.S.S.), the Fonds der Chemischen Industrie and the Freistaat Thüringen. We also thank Vera Cimrová (cyclic voltammetry: Institute of Macromolecular Chemistry, Academy of Science of the Czech Republic, Prague, Czech Republic) and Beate Lentvogt (elemental analysis) for the help with the respective measurements.

Supporting Information Available: Text giving full experimental details and characterization of the aromatic dibromides (**1**–**7**), bis(terpyridines) (**M1**–**M7**) and metallo-polymers (**P1**–**P7**, **R1**, **R2**) including reaction schemes and structures, and figures showing NMR and MALDI–TOF mass spectra of bis(terpyridines) (**M1**–**M7**). This material is available free of charge via the Internet at http://pubs.acs.org.

References and Notes

(1) Lehn, J. M. *Angew. Chem., Int. Ed.* **1988**, *27*, 89–112.
(2) Schubert, U. S.; Hofmeier, H.; Newkome, G. R. *Modern Terpyridine Chemistry*; VCH Wiley: Weinheim, Germany, 2006.
(3) Lehn, J.-M. *Supramolecular Chemistry—Concepts and Chemistry*; VCH Wiley: Weinheim, Germany, 1995.
(4) Balzani, V.; Juris, A.; Venturi, M.; Campagna, S.; Serroni, S. *Chem. Rev.* **1996**, *96*, 759–833.
(5) Eisenbach, C. D.; Schubert, U. S. *Macromolecules* **1993**, *23*, 7372–7374.
(6) Newkome, G. R.; Wang, P. S.; Moorefield, C. N.; Cho, T. J.; Mohapatra, P. P.; Li, S. N.; Hwang, S. H.; Lukoyanova, O.; Echegoyen, L.; Palagallo, J. A.; Iancu, V.; Hla, S. W. *Science* **2006**, *312*, 1782–1785.
(7) Hofmeier, H.; Schmatloch, S.; Wouters, D.; Schubert, U. S. *Macromol. Chem. Phys.* **2003**, *204*, 2197–2203.
(8) Lohmeijer, B. G. G.; Schubert, U. S. *Macromol. Chem. Phys.* **2003**, *204*, 1072–1078.
(9) Dobrawa, R.; Lysetska, M.; Ballester, P.; Grüne, M.; Würthner, F. *Macromolecules* **2005**, *38*, 1315–1325.
(10) Dobrawa, R.; Würthner, F. *J. Polym. Sci., Part A: Polym. Chem.* **2005**, *43*, 4981–4995.
(11) Schubert, U. S.; Eschbaumer, C. *Angew. Chem., Int. Ed.* **2002**, *41*, 2893–2926.
(12) Bonnet, S.; Collin, J. P.; Koizumi, M.; Mobian, P.; Sauvage, J. P. *Adv. Mater.* **2006**, *18*, 1239–1250.
(13) Schmatloch, S.; van den Berg, A. M. J.; Alexeev, A. S.; Hofmeier, H.; Schubert, U. S. *Macromolecules* **2003**, *36*, 9943–9949.
(14) Schubert, U. S.; Schmatloch, S.; Precup, A. A. *Des. Monomers Polym.* **2002**, *5*, 211–221.
(15) Schubert, U. S.; Hien, O.; Eschbaumer, C. *Macromol. Rapid Commun.* **2000**, *21*, 1156–1161.
(16) Winter, A.; Friebe, C.; Hager, M. D.; Schubert, U. S. *Macromol. Rapid Commun.* **2008**, *29*, 1679–1686.
(17) Hissler, M.; El-ghayoury, A.; Harriman, A.; Ziessel, R. *Angew. Chem., Int. Ed.* **1998**, *37*, 1717–1720.
(18) Sauvage, J. P.; Collin, J. P.; Chambron, J. C.; Guillerez, S.; Coudret, C.; Balzani, V.; Barigelletti, F.; Decola, L.; Flamigni, L. *Chem. Rev.* **1994**, *94*, 993–1019.
(19) Dobrawa, R.; Würthner, F. *Chem. Commun.* **2002**, 1878–1879.
(20) Flores-Torres, S.; Hutchison, G. R.; Soltzberg, L. J.; Abruna, H. D. *J. Am. Chem. Soc.* **2006**, *128*, 1513–1522.
(21) Erkkila, K. E.; Odom, D. T.; Barton, J. K. *Chem. Rev.* **1999**, *99*, 2777–2795.
(22) Barigelletti, F.; Flamigni, L. *Chem. Soc. Rev.* **2000**, *29*, 1–12.
(23) Chen, Y. Y.; Tao, Y. T.; Lin, H. C. *Macromolecules* **2006**, *39*, 8559–8566.
(24) Winter, A.; Friebe, C.; Chiper, M.; Hager, M. D.; Schubert, U. S. *J. Polym. Sci., Part A: Polym. Chem.* **2009**, *47*, 4083–4098.

(25) Manners, I. *Science* **2001**, *294*, 1664–1666.
(26) Constable, E. C.; Thompson, A. M. W. C. *J. Chem. Soc., Chem. Commun.* **1992**, 617–619.
(27) Vellis, P. D.; Mikroyannidis, J. A.; Lo, C. N.; Hsu, C. S. *J. Polym. Sci., Part A: Polym. Chem.* **2008**, *46*, 7702–7712.
(28) Chen, Y. Y.; Lin, H. C. *J. Polym. Sci., Part A: Polym. Chem.* **2007**, *45*, 3243–3255.
(29) Parameswar, K. I.; Beck, B.; Weder, C.; Rowan, S. J. *Chem. Commun.* **2005**, 319–321.
(30) Yu, S.-C.; Kwok, C.-C.; Chan, W.-K.; Che, C.-M. *Adv. Mater.* **2003**, *15*, 1643–1647.
(31) Huang, F.; Wu, H.; Wang, D.; Wang, W.; Cao, Y. *Chem. Mater.* **2004**, *16*, 708–712.
(32) Winter, A.; Egbe, D. A. M.; Schubert, U. S. *Org. Lett.* **2007**, *9*, 2345–2348.
(33) Winter, A.; Friebe, C.; Hager, M. D.; Schubert, U. S. *Eur. J. Org. Chem.* **2009**, 801–809.
(34) Roncali, J. *Chem. Rev.* **1997**, *97*, 173–205.
(35) Cheng, Y. J.; Yang, S. H.; Hsu, C. S. *Chem. Rev.* **2009**, *109*, 5868–5923.
(36) Förster, T. *Annal. Phys.* **1948**, *6*, 55–75.
(37) Lakowicz, J. R. *Principles of Fluorescence Spectroscopy*; Kluwer Academic/Plenum: New York, 1999.
(38) Santoni, M.-P.; Medlycott, E. A.; Hanan, G. S.; Hasenknopf, B.; Proust, A.; Nastasi, F.; Campagna, S.; Chiorboli, C.; Argazzi, R.; Scandola, F. *Dalton Trans.* **2009**, 3964–3970.
(39) Winter, A.; van den Berg, A. M. J.; Hoogenboom, R.; Kickelbick, G.; Schubert, U. S. *Synthesis* **2006**, 2873–2878.
(40) Wang, J. H.; Hanan, G. S. *Synlett* **2005**, 1251–1254.
(41) Smith, C. B.; Raston, C. L.; Sobolev, A. N. *Green Chem* **2005**, *7*, 650–654.
(42) Pilgram, K.; Zupan, M.; Skiles, R. *J. Heterocycl. Chem.* **1970**, *7*, 629–640.
(43) Bartholome, D. Ph.D. Thesis. Friedrich-Schiller-University Jena, Jena, Germany, **2007**.
(44) Karsten, B. P.; Viani, L.; Gierschner, J.; Cornil, J.; Janssen, R. A. J. *J. Phys. Chem.* **2008**, *112*, 10764–10773.
(45) Huo, L. J.; Tan, Z. A.; Zhou, Y.; Zhou, E. J.; Han, M. F.; Li, Y. F. *Macromol. Chem. Phys.* **2007**, *208*, 1294–1300.
(46) Ahmed, A. M.; Feast, W. J.; Tsibouklis, J. *Polymer* **1993**, *34*, 1297–1302.
(47) Shen, P.; Sang, G. Y.; Lu, J. J.; Zhao, B.; Wan, M. X.; Zou, Y. P.; Li, Y. F.; Tan, S. T. *Macromolecules* **2008**, *41*, 5716–5722.
(48) Shahid, R. A. Ph.D. Thesis. Friedrich-Schiller-University Jena, Jena, Germany, **2005**.
(49) Shahid, M.; Shahid, R. A.; Klemm, E.; Sensfuss, S. *Macromolecules* **2006**, 7844–7853.
(50) Wild, A.; Friebe, C.; Winter, A.; Hager, M. D.; Grummt, U. W.; Schubert, U. S. *Eur. J. Org. Chem.* **2010**, DOI: 10.1002/ejoc.200901112.
(51) In order to obtain an analytical pure sample, a larger number of precipitation steps was required and, thus, a lower isolated yield compared with the other systems was observed.
(52) Yuan, S. C.; Chen, H. B.; Zhang, Y.; Pei, J. *Org. Lett.* **2006**, *8*, 5700–5704.
(53) Wild, A.; Schlütter, F.; Pavlov, G. M.; Friebe, C.; Festag, G.; Winter, A.; Hager, M. D.; Schubert, U. S. *Macromol. Rapid Commun.* **2010**, DOI:10.1002/marc.200900889.
(54) Janitetz, S.; Bradley, D. D. C.; Grelly, M.; Giebeler, C.; Inbasekaran, M.; Woo, E. P. *Appl. Phys. Lett.* **1998**, *73*, 2453–2468.
(55) Chiper, M. Ph.D. Thesis. Eindhoven University of Technology, Eindhoven, The Netherlands, **2008**.
(56) Ashraf, R. S.; Shahid, M.; Klemm, E.; Al-Ibrahim, M.; Sensfuss, S. *Macromol. Rapid Commun.* **2006**, *27*, 1454–1459.
(57) Wu, W.-C.; Lee, W.-Y.; Pai, C.-L.; Chen, W.-C.; Tuan, C.-S.; Lin, J.-L. *J. Polym. Sci., Part B: Polym. Phys.* **2006**, *45*, 67–78.
(58) The synthesis and characterization of the homo polymers **P8** and **P9** based on the donor-bridged bis(terpyridines) **MD1** and **MD2**, respectively, is shown elsewhere.[53]
(59) Spehar-Deleze, A. M.; Pellegrin, Y.; Keyes, T. E.; Forster, R. J. *Electrochem. Commun.* **2008**, *10*, 984–986.
(60) Kelch, S.; Rehahn, M. *Macromolecules* **1999**, *32*, 5818–5828.